ACI STRUCTURAL JOURNAL TECHNICAL PAPER

Title no. 107-S12

# Evaluation of Steel Fiber Reinforcement for Punching Shear Resistance in Slab-Column Connections—Part II: Lateral Displacement Reversals

by Min-Yuan Cheng and Gustavo J. Parra-Montesinos

*Results from an experimental investigation aimed at evaluating the seismic behavior of steel fiber-reinforced concrete slab-column connections are presented. Two approximately half-scale slab-column subassemblies were tested under combined gravity load and lateral displacement reversals to evaluate the ability of fiber reinforcement to increase the connection punching shear strength and deformation capacity. The connection of one specimen featured high-strength (2300 MPa [334 ksi]) hooked steel fibers in a 1.5% volume fraction, while the other connection was reinforced with regular strength (1100 MPa [160 ksi]) hooked steel fibers, also in a 1.5% volume fraction. The two connection subassemblies were subjected to displacement cycles of up to 5% drift in combination with gravity shear ratios as large as 5/8. While the connection with regular strength hooked fibers exhibited substantial punching shear-related damage at the end of the test, no significant damage could be observed in the connection with high-strength fibers. A combined shear stress due to direct shear and unbalanced moment of (1/3) $\sqrt{f'_c}$ (MPa) (4 $\sqrt{f'_c}$ [psi]) represented a limit below which a rotation capacity of at least 0.05 rad can be expected in connections constructed with either of the two fiber-reinforced concretes evaluated. In terms of gravity shear ratio, the data suggest that a gravity shear ratio of 1/2 is a safe upper limit for ensuring a minimum drift capacity of 4% drift.*

**Keywords**: punching shear; reinforcement; steel fibers.

## INTRODUCTION

Slab-column frame systems are widely used in reinforced concrete construction because of their low cost, space usage flexibility, and architectural appearance. When used in regions of high seismicity, slab-column frames are combined with laterally stiffer and stronger systems, such as structural walls or special moment resisting frames. Although typically not designed to contribute to lateral load resistance, slab-column frames must be capable of sustaining gravity loads while undergoing earthquake-induced displacements.

Experimental research (Pan and Moehle 1988; Hwang and Moehle 1993) and post-earthquake observations (Hueste and Wight 1997) have provided clear evidence that slab-column connections are susceptible to punching shear failures under the action of earthquake-induced deformations. Further, good correlation has been found between drift capacity (lateral interstory displacement divided by story height) and the intensity of connection shear due to gravity loads, typically expressed as the ratio between direct shear induced by gravity loads and nominal punching shear strength. This ratio is referred to as the gravity shear ratio.

To account for the relationship between drift capacity and gravity shear ratio in slab-column frames, Section R21.13.6 of the ACI Building Code (ACI Committee 318 2008) includes a drift versus gravity shear ratio interaction diagram to determine whether shear reinforcement is needed in the connections (Fig. 1). For a gravity shear ratio of 0.3, a 2% drift capacity is assumed, whereas a gravity shear ratio of 1/2 corresponds to a 1% drift capacity. Alternatively, a stress-based check can be performed, in which the combined shear stress due to direct shear and unbalanced moment is calculated and compared with the nominal shear strength of the connection. In practice, however, the application of either method often leads to the use of shear reinforcement in connections of slab-column frames located in earthquake-prone regions.

Although several types of shear reinforcement in slab-column connections have been investigated, such as bent-up bars, shearheads, and hoops (refer to, for example, Elstner and Hognestad [1956], Corley and Hawkins [1968], Hawkins et al. [1974], Hanna et al. [1975], Islam and Park [1976], and Robertson et al. [2002]), shear stud reinforcement (Dilger and Ghali 1981) has become the preferred option for structural engineers and contractors in the past few years. In this research, however, an alternative reinforcement solution is investigated, which consists of the use of discontinuous, randomly oriented steel fibers in the slab-column connection region.

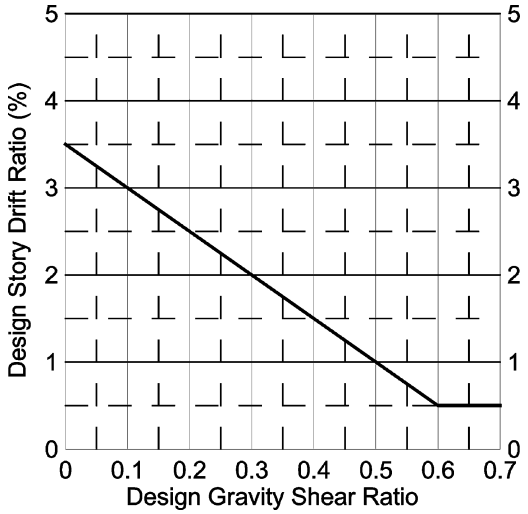


*Fig. 1—Drift versus gravity shear ratio interaction diagram in ACI Building Code (ACI Committee 318 2008).*

*ACI Structural Journal*, V. 107, No. 1, January-February 2010.
MS No. S-2009-039.R1 received February 11, 2009, and reviewed under Institute publication policies.  Pertinent discussion including author's closure, if any, will be published in the November-December 2010 *ACI Structural Journal* if the discussion is received by July 1, 2010.

**Min-Yuan Cheng** *is a Structural Engineer at Cary Kopzcynski and Company, Bellevue, WA. He received his BS in marine engineering from National Sun-Yat-Sen University, Taiwan; his MS in civil engineering from National Cheng Kung University, Tainan City, Taiwan; and his PhD in civil engineering from the University of Michigan, Ann Arbor, MI.*

*ACI member* **Gustavo J. Parra-Montesinos** *is an Associate Professor at the University of Michigan. He is Secretary of ACI Committee 335, Composite and Hybrid Structures, and a member of the ACI Publications Committee; ACI Committees 318, Structural Concrete Building Code; and Joint ACI-ASCE Committee 352, Joints and Connections in Monolithic Concrete Structures. His research interests include the behavior and design of reinforced concrete, fiber-reinforced concrete, and composite steel-concrete structures.*

To the authors' knowledge, Diaz and Durrani (1991) were the only researchers that, prior to this research, evaluated the use of fiber-reinforced concrete in slab-column connections subjected to combined gravity load and lateral displacement reversals. In their research, three interior and three exterior connection subassemblies were tested under a relatively low gravity shear ratio (approximately 0.2). Steel crimped fibers in volume ratios of 0.38, 0.76, and 1.11% were used. All three exterior connection subassemblies, as well as the interior connections with either 0.76% or 1.11% fiber volume fraction, were able to sustain drift cycles of up to 7% drift. On the other hand, the interior connection with 0.38% volume fraction of steel fibers failed by punching at 6% drift.

Although the results obtained by Diaz and Durrani (1991) provide strong evidence of the ability of steel fiber reinforcement to enhance the seismic behavior of slab-column connections, their application is limited to connections with low gravity shear ratios. Thus, the research presented herein was aimed at investigating the ability of fiber reinforcement to increase punching shear resistance and deformation capacity of slab-column connections when subjected to moderate levels of gravity shear ratio (up to approximately 5/8) combined with lateral displacement reversals.

## RESEARCH SIGNIFICANCE

The seismic behavior of slab-column connections constructed with fiber-reinforced concrete is little known. This paper provides new information on the ability of fiber reinforcement to enhance punching shear strength and deformation capacity of slab-column connections when subjected to combined gravity load and lateral displacement reversals. In particular, new data are provided with respect to the interaction between connection shear stress demand and rotation capacity, as well as between gravity shear ratio and drift capacity in fiber-reinforced concrete slab-column connections.

## RESEARCH DESCRIPTION

This research focused on the evaluation of the seismic behavior of fiber-reinforced concrete slab-column connections. Two approximately half-scale slab-column subassemblies, Specimens SU1 and SU2, were tested under simulated gravity load and lateral displacement reversals. The connections in these two specimens were constructed with the two fiber-reinforced concretes that led to the best performance in terms of punching shear strength and ductility in slabs subjected to monotonically increased load, as described in the companion paper (Cheng and Parra-Montesinos 2010).

### Description of test specimens

The main features of the test specimens are summarized in Table 1. The slab in each specimen was 2.74 x 2.74 x 0.1 m (108 x 108 x 4 in.), as shown in Fig. 2. The slab-column subassemblies were pinned supported at the column base. The four corners of the slab were supported by four steel arms designed as rollers to restrain vertical displacement while allowing lateral displacement and rotation in the loading direction. Steel C-shape members, connected to the steel arms, were fastened above and below the slab through bolts to restrain vertical displacement along the slab perimeter (Fig. 2).

The column in each subassembly had a 31 cm (12 in.) square cross section and extended 89 and 102 cm (35 and 40 in.) above and below the top and bottom slab surfaces, respectively. The column ends were connected to steel fixtures for attachment to the test setup, which resulted in a total story height (distance between applied displacement and bottom pinned support) of approximately 2.54 m (100 in.). Lateral displacement reversals were applied at the top of the column through a 450 kN (100 kip) hydraulic actuator.

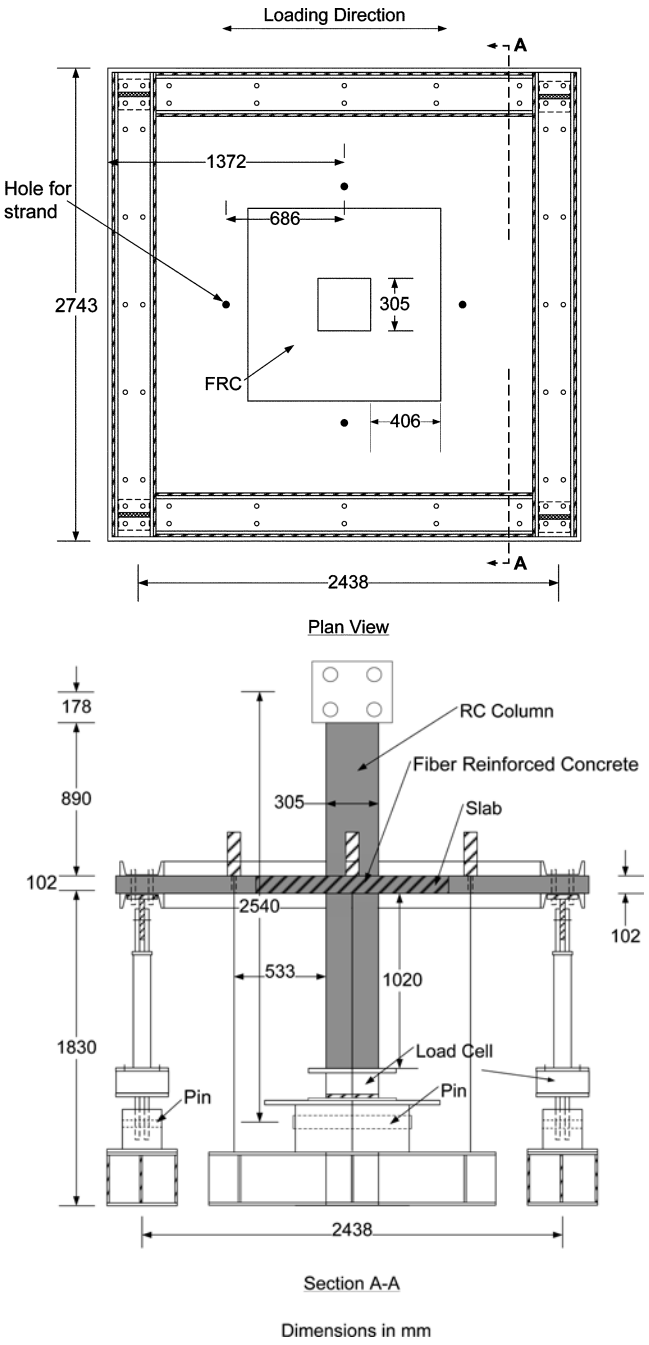


*Fig. 2—Geometry of test specimens. (Note: 1 mm = 0.0394 in.)*

**Table 1—Main features of test specimens**

| Specimen | Dimensions | | | Fiber reinforcement* | | | | Slab reinforcement | | | |
|---|---|---|---|---|---|---|---|---|---|---|---|
| | | | | | | | | Column strip | | Effective width† | |
| | Slab, m | $d$, mm | Column, m | $L_f$, mm | $d_f$, mm | $f_u$, MPa | $V_f$, % | $\rho_{top}$, % | $\rho_{bot}$, % | $\rho_{top}$, % | $\rho_{bot}$, % |
| SU1 | 2.74 x 2.74 x 0.1 | 83 | 0.3 x 0.3 | 30 | 0.38 | 2300 | 1.5 | 0.52 | 0.34 | 0.57 | 0.46 |
| SU2 | | | | 30 | 0.55 | 1100 | 1.5 | | | | |

*Only in 1.12 m slab central region.
†Effective width is column width + 3 (slab thickness).
Note: $d$ is slab effective depth, $L_f$ is fiber length, $d_f$ is fiber diameter, $f_u$ is fiber strength, $V_f$ is fiber volume fraction, ρ is reinforcement ratio; 1 mm = 0.0394 in.; 1 m = 39.4 in.; and 1 MPa = 0.145 ksi.

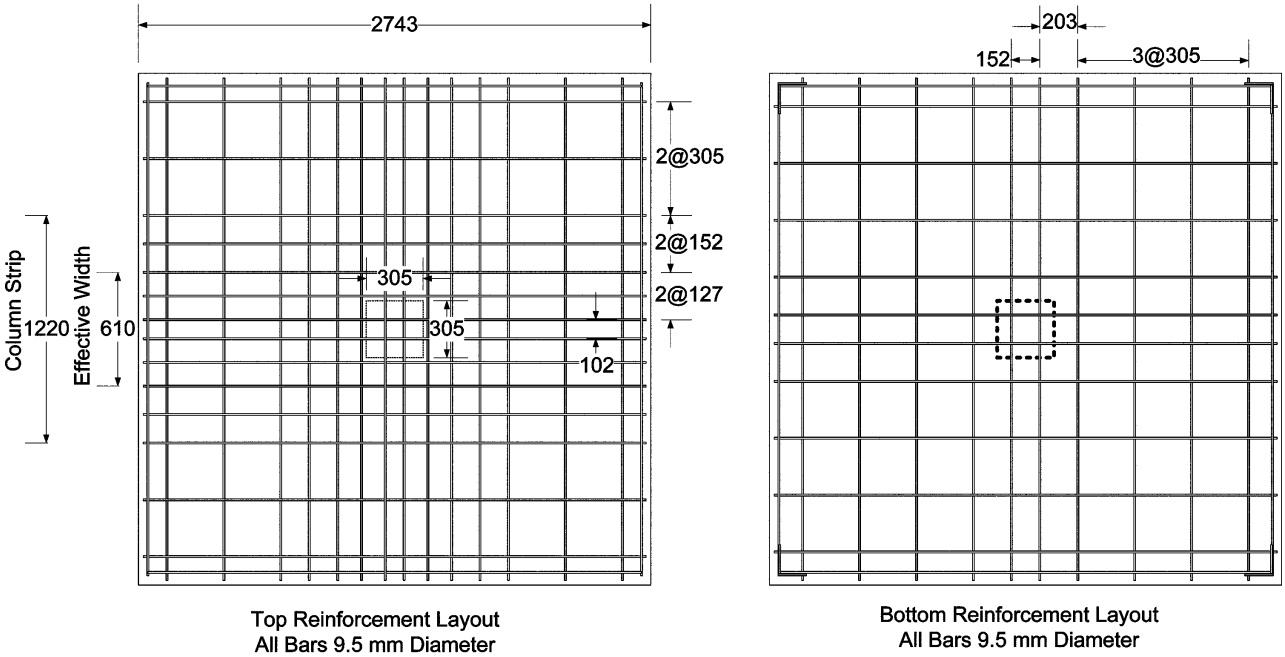


*Fig. 3—Slab reinforcement layout. (Note: 1 mm = 0.0394 in.)*

The slab of Specimens SU1 and SU2, with nominally "identical" reinforcement layout, was designed as being part of a floor system subjected to a uniform gravity load. The intensity of the gravity load was determined to induce an average shear stress of (1/6) $\sqrt{f_c'}$ (MPa) (2 $\sqrt{f_c'}$ [psi]) at the critical section of the connection ($d$/2 from the column faces), where $f_c'$ is the concrete cylinder strength. For the connection configuration tested, this target shear stress corresponded to a gravity shear ratio of 1/2. The effective slab depth $d$ for the reinforcement parallel to the loading direction was equal to 83 mm (3.25 in.). Detailed information about the design of the test specimens can be found elsewhere (Cheng and Parra-Montesinos 2009).

The slab reinforcement layout for Specimens SU1 and SU2 is shown in Fig. 3. No. 10M (9.5 mm [3/8 in.] diameter), Grade 420M (60) bars were selected as slab flexural reinforcement for both specimens. Two continuous bottom bars passing through the column in each principal direction were provided to satisfy the ACI Code requirement against progressive collapse outlined in Section 13.3.8.5 (ACI Committee 318 2008). Also, the top reinforcement provided within the effective slab width (column width + 3$h$, where $h$ is the slab thickness) exceeded 50% of the total reinforcement provided within the column strip, as specified in ACI Code Section 21.3.6.3 (ACI Committee 318 2008).

Based on the flexural capacity of the slab and applied gravity load, the column was designed to remain elastic throughout the test. Eight No. 16M (16 mm [5/8 in.] diameter) Grade 420M bars were used as column longitudinal reinforcement, enclosed by No. 13M (13 mm [1/2 in.] diameter) Grade 420M hoops at 7.5 cm (3 in.) spacing. No ties were placed within the joint region (intersection between slab and column); the closest ties were positioned 2.5 cm (1 in.) above the slab and 3.2 cm (1.25 in.) below the lowest slab bottom reinforcement.

The connection of Specimen SU1 was reinforced with high-strength (2300 MPa [334 ksi]) hooked steel fibers in a 1.5% volume ratio, while the connection of Specimen SU2 was reinforced with regular strength (1100 MPa [160 ksi]) hooked fibers, also in a 1.5% volume fraction. In the two test specimens, fiber-reinforced concrete was used only in the 112 cm (44 in.) square region at the center of the slab. The perimeter of the fiber-reinforced concrete region was thus located at four times the slab thickness from each column face. Based on the applied gravity load and expected slab flexural strength, a peak combined shear stress less than (1/6) $\sqrt{f_c'}$ (MPa) (2 $\sqrt{f_c'}$ [psi]) was expected at the interface between the fiber-reinforced concrete and regular concrete regions of the slab.

## TEST PROCEDURE

Simulated gravity load, in addition to the slab self-weight, was applied through four prestressing strands tensioned by hydraulic jacks, each located at approximately mid-length

between the column face and the slab edge (Fig. 2). The force in the prestressing strands was dictated by the target average shear stress in the connection critical perimeter of $(1/6)\sqrt{f_c'}$ (MPa) ($2\sqrt{f_c'}$ [psi]), where the concrete strength $f_c'$ was obtained through cylinder tests performed one day prior to each test. Connection gravity shear was monitored through a load cell located underneath the column (Fig. 2). Once the desired gravity load was attained, the hydraulic pressure in the hydraulic jacks was locked. Because of load redistribution during testing, primarily due to concrete cracking and reinforcement yielding, the connection shear was checked between drift cycles and the force in the prestressing strands adjusted, if needed. No attempt was made to keep the gravity shear ratio constant during application of each lateral displacement cycle.

Displacement cycles of increasing magnitude were applied to the test specimens. Originally, a peak drift demand of 4% was intended. Given the fact that no significant damage was observed in the test connections at this drift level, however, additional drift cycles were applied, in combination with an increase in the target gravity shear ratio to 5/8. The applied lateral displacement histories for Specimens SU1 and SU2 are shown in Fig. 4(a) and (b), respectively.

**Table 2—Material properties**

| Specimen | Concrete | | Steel (No. 10M bars) | |
|---|---|---|---|---|
| | Type | Strength, MPa | Yield strength, MPa | Ultimate strength, MPa |
| SU1 | Fiber reinforced | 58.5 | 528 | 801 |
| | Plain | 33.4 | | |
| SU2 | Fiber reinforced | 47.8 | | |
| | Plain | 50.2 | | |

Note: 1 MPa = 0.145 ksi.

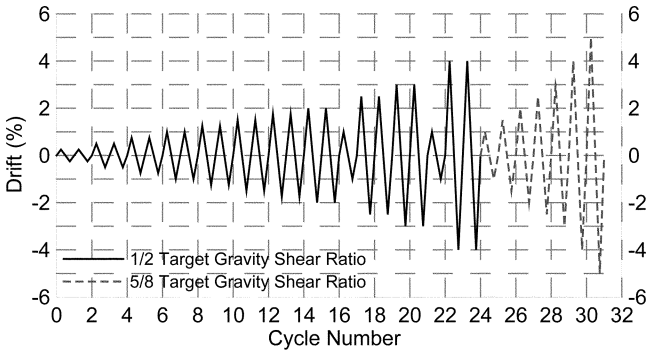


*(a) Specimen SU1*

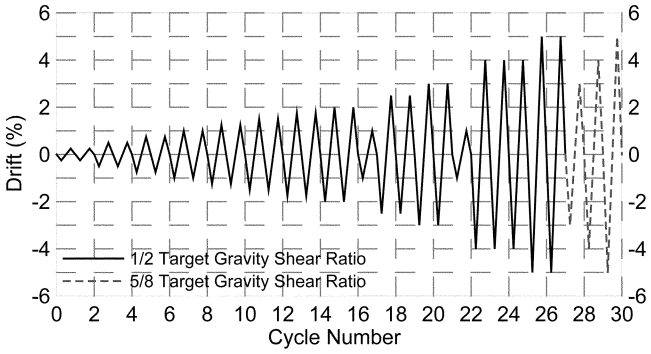


*(b) Specimen SU2*

*Fig. 4—Lateral displacement history.*

## MATERIAL PROPERTIES

### Fiber-reinforced concrete and regular concrete

Both fiber-reinforced concretes were mixed in the Structural Engineering Laboratory at the University of Michigan with concrete proportions by weight of 1:0.48:1.45:1.55 (Type III cement: water: coarse aggregate: sand). Crushed limestone with a 13 mm (1/2 in.) maximum size was used. For the rest of the slab, ready mixed concrete with a specified 28-day compressive strength of 34.5 MPa (5000 psi) was provided by a local concrete supplier. The placing of regular concrete was performed immediately after fiber-reinforced concrete was cast in the connection region.

The compressive strength of the fiber-reinforced concrete and regular concrete used in the slabs was evaluated through 10 x 20 cm (4 x 8 in.) cylinder tests. The compressive strengths obtained from the cylinder tests are listed in Table 2. Beam specimens with dimensions of 15 x 15 x 51 cm (6 x 6 x 20 in.) were also prepared for each fiber-reinforced concrete material (three beams for Specimen SU1 and two beams for Specimen SU2). All beams were tested under third-point loading, according to ASTM 1609-05. The results between the beams tested for each material were relatively consistent (ratio between minimum and maximum strength at a given deflection greater than 0.75). Figure 5 shows the average load versus deflection response for the beam specimens corresponding to Specimens SU1 and SU2. The fiber-reinforced concrete beams corresponding to Specimen SU1 clearly exhibited a deflection hardening behavior after first cracking and up to a deflection of approximately 0.7 mm (0.027 in.) (beam span length/730), followed by a gradual decrease in strength. On the other hand, the behavior of the fiber-reinforced concrete beams corresponding to Specimen SU2 could be considered a transition between deflection softening and deflection hardening behavior.

### Reinforcing steel

Steel bars used in Specimens SU1 and SU2 were ordered and shipped together. All reinforcing bars were made of Grade 420M (60) steel. Results from direct tensile tests on the slab reinforcing steel are summarized in Table 2.

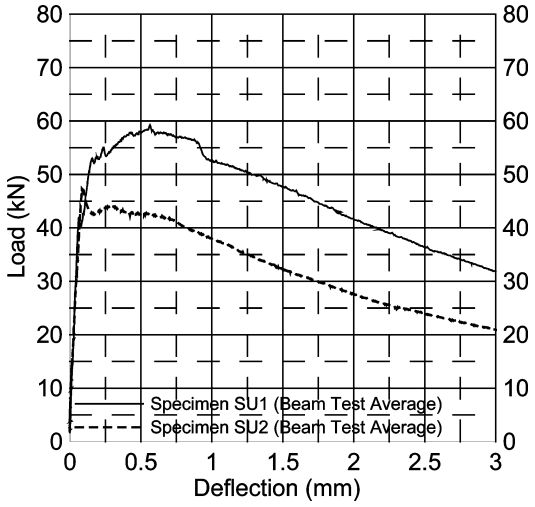


*Fig. 5—Load versus deflection response obtained from ASTM 1609 beam tests. (Note: 1 kN = 0.225 kips; 1 mm = 0.0394 in.)*

## EXPERIMENTAL RESULTS

### Overall behavior

*Specimen SU1*—The load versus displacement relationship for Specimen SU1, with high-strength hooked fibers in a 1.5% volume fraction, is shown in Fig. 6(a). As can be seen, the specimen exhibited a stable hysteresis behavior up to 4% drift when subjected to a target gravity shear ratio of 1/2, behavior that was dominated by the flexural response of the slab. Strain gauge readings indicated flexural yielding of the slab for drift cycles greater than 2%. Connection rotation data, however, suggest that slab flexural yielding initiated at lower drifts (approximately 1%). At 4% drift, slab flexural yielding had spread transversely over a distance of 4*h* from each column lateral face, where *h* is the slab thickness. At this displacement level, only minor damage was observed in the connection region, which was characterized by a few narrow flexural cracks.

The applied connection shear ratio in Specimen SU1 was checked against the target ratio of 1/2 at the beginning of each displacement cycle and the force in the prestressing strands adjusted, if needed. As shown in Fig. 7(a), variations in connection shear occurred during each displacement cycle due to force redistribution from the connection to the vertical steel arms supporting the slab corners. The decrease in gravity shear became particularly important during the latter drift cycles, leading to a drop of up to 50% in connection gravity shear during the cycles at 4% drift. Upon completion of each loading cycle, however, the applied gravity shear was close to the target value.

Because little damage was observed in Specimen SU1 at the end of the 4% drift cycle under a target gravity shear ratio of 1/2, a decision was made to increase the target gravity shear ratio to 5/8 and apply additional loading cycles, as shown in Fig. 4(a). The load-versus-drift response for this second test on Specimen SU1 is shown in Fig. 6(b). As can be seen, the hysteresis behavior of Specimen SU1 under a target gravity shear ratio of 5/8 was similar to that under a 1/2 target shear ratio. The relatively wide hysteresis loops up to 5% drift at such a high connection shear are a clear indication of large deformation and energy dissipation capacity. As in the test under a 1/2 gravity shear ratio, a reduction in connection shear was noticed during the application of lateral displacements (Fig. 7(b)). This shear decrease ranged from 10% for the cycle at 3% drift to 30% for the cycle at 5% drift. At the end of the test, Specimen SU1 showed little damage in the connection region.

To evaluate the residual punching shear capacity of Specimen SU1, a monotonically increased vertical load was applied on the slab after the completion of the lateral displacement cycles. This was achieved by increasing the

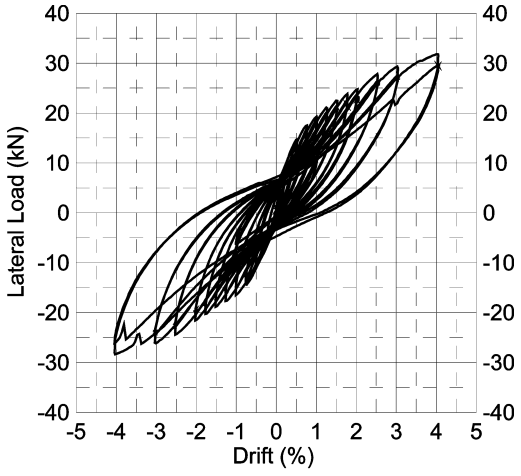


a) 1/2 Target gravity shear ratio

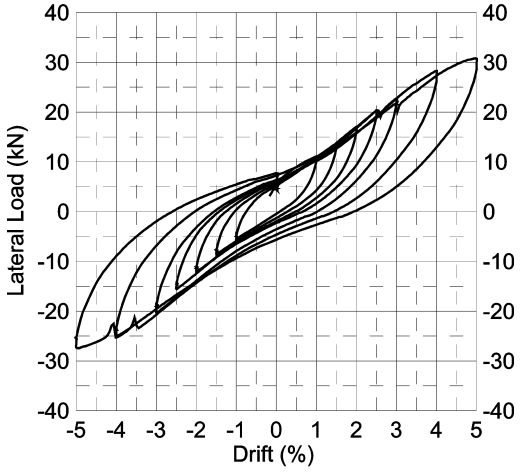


b) 5/8 Target gravity shear ratio

*Fig. 6—Load versus drift response (Specimen SU1). (Note: 1 kN = 0.225 kips.)*

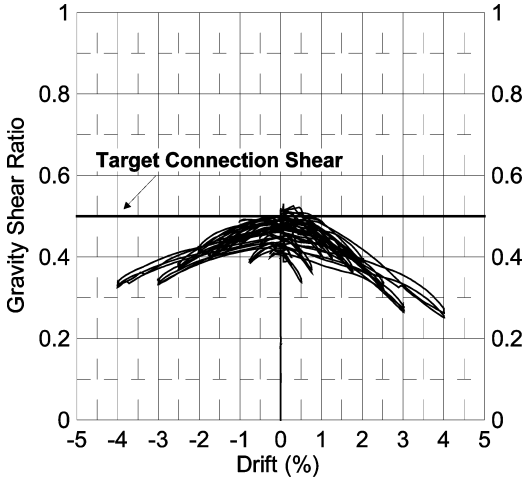


a) 1/2 Target gravity shear ratio

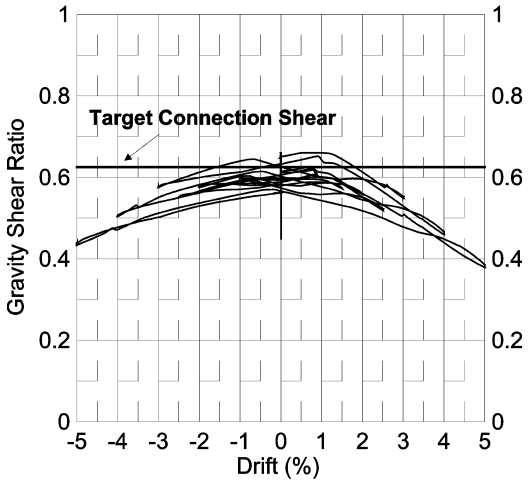


b) 5/8 Target gravity shear ratio

*Fig. 7—Gravity shear ratio history (Specimen SU1).*

force in the four prestressing strands connected to the slab. The maximum force applied to the slab was limited by the capacity of the loading system (445 kN [100 kips]), which led to a peak connection shear force of 334 kN (75 kips). This connection shear corresponded to an average shear stress of approximately (1/3) $\sqrt{f_c'}$ (MPa) ($4\sqrt{f_c'}$ [psi]) or a gravity shear ratio of 1.0. The slab of Specimen SU1 was then saw-cut after completion of the tests. Although some minor inclined cracks were found near the connection region, most of the damage was in the form of flexural cracks.

*Specimen SU2*—Some problems were encountered during the test of Specimen SU2, whose connection was reinforced with a 1.5% volume fraction of regular strength hooked steel fibers. First, the data acquisition system stopped recording data during the first cycle at 4% drift. Because the system was restarted upon completion of the second cycle at 4% drift, a third cycle at 4% drift was then applied to record the specimen behavior over one full cycle at this drift level. Another problem encountered during the test of Specimen SU2 was related to the pin-connection at the column base. During the specimen setup process, a steel plate was inserted to restrain large rotations of the pin connection at the bottom of the column. This steel plate was accidentally left in place during the test, which resulted in a rotational restrain at the base of the column for drifts greater than 2.5%. After completion of the test, several displacement cycles at various drift levels were applied with and without the steel plate to quantify its effect on the measured load. It was determined that the restrain provided by the steel plate led to an increase in lateral force of up to 35% during the cycles at 4 and 5% drift under a target gravity shear ratio of 1/2. This force difference increased up to 45% when the specimen was subjected to a target gravity shear ratio of 5/8. The load versus drift response was then adjusted accordingly. Detailed information about the correction of the load history of Specimen SU2 can be found elsewhere (Cheng and Parra-Montesinos 2009).

The adjusted lateral load versus drift response for Specimen SU2 is shown in Fig. 8(a). As can be seen, the response was similar to that of Specimen SU1 up to 4% drift when subjected to a target gravity shear ratio of 1/2. Flexural yielding in Specimen SU2 was first detected through strain gauge data during the first cycle at 1.5% drift. At 4% drift, yielding had spread transversely over approximately 4*h* from each column lateral face, as in Specimen SU1. During the

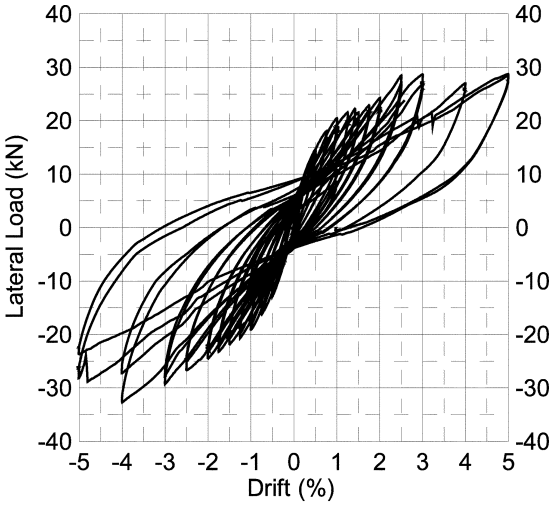


**a) 1/2 Target gravity shear ratio**

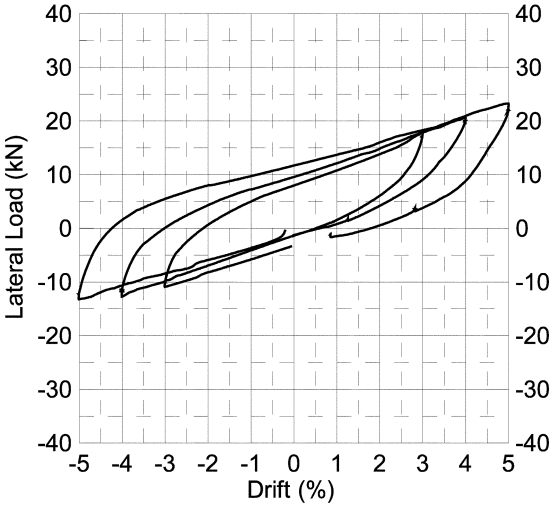


**b) 5/8 Target gravity shear ratio**

*Fig. 8—Lateral load versus drift response (Specimen SU2). (Note: 1 kN = 0.225 kips.)*

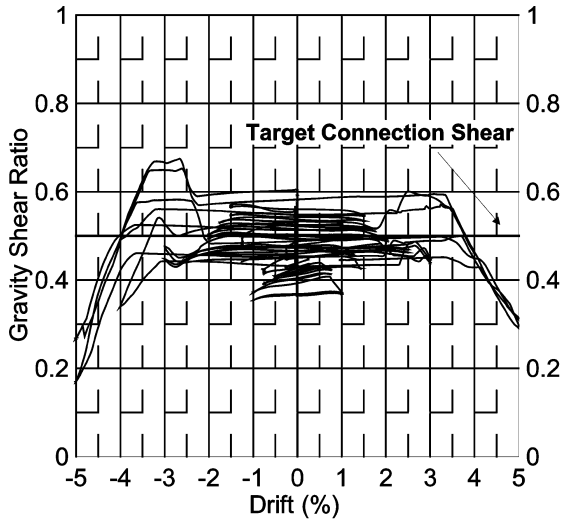


**a) 1/2 Target gravity shear ratio**

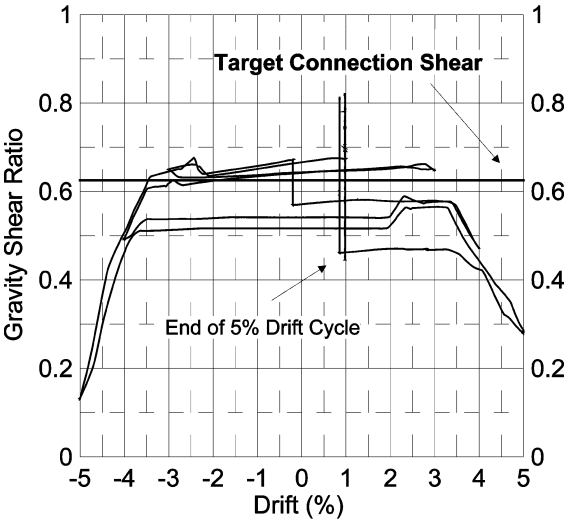


**b) 5/8 Target gravity shear ratio**

*Fig. 9—Gravity shear ratio history (Specimen SU2).*

repeated negative half-cycle at 4% drift, however, the strength of Specimen SU2 dropped by nearly 20%. This was believed to have been caused by the initiation of punching shear-related damage. Further increase in drift from 4% to 5% led to a relatively minor decrease in strength for the first half-cycle in the negative loading direction. When subjected to the repeated cycle at 5% drift, an additional decrease in strength occurred for the negative loading direction.

Specimen SU2 was able to sustain the applied gravity load, targeted at a 1/2 gravity shear ratio, up to 5% drift. As shown in Fig. 9(a), the applied gravity load was greater than or equal to the target value for drift levels of up to 4%. For larger drifts, however, the applied gravity load decreased below the target value.

After the cycle to 5% drift was completed on Specimen SU2, the applied gravity shear ratio was increased to 5/8 and further displacement cycles were applied (Fig. 4(b)). Under this gravity shear ratio, the lateral resistance was substantially lower than that observed during the test under a 1/2 target shear ratio, particularly for the negative loading direction (Fig. 8(b)). Specimen SU2, however, was still able to sustain the applied gravity shear during the cycle to 3% drift (Fig. 9(b)). For the loading cycles to 4 and 5% drift, a decrease in the applied gravity shear for drifts greater than 3.5% was observed, similar to the previous test under a 1/2 gravity shear. This decrease in gravity load became severe during the cycle at 5% drift. At the end of the test, the connection of Specimen SU2 exhibited extensive punching shear-related damage and some concrete spalling, as shown in Fig. 10.

To evaluate the residual punching shear capacity of the connection in Specimen SU2, the connection shear was increased to approximately 200 kN (45 kips) after completion of the lateral displacement cycles. This shear force corresponded to a gravity shear ratio of 0.68. The fact that the connection of Specimen SU2 was capable of sustaining such high gravity shear ratio showed that it still possessed adequate gravity load carrying capacity even though significant punching shear-related damage could be observed at the end of the test.

## Connection rotations

Connection rotations were measured through linear potentiometers along the slab centerline, parallel to the loading direction, at a distance of 1*d* from the column faces.

*Fig. 10—Connection of Specimen SU2 at end of lateral displacement cycles.*

The initial application of a gravity load (1/2 gravity shear ratio) led to a rotation of approximately 0.0025 rad on both sides of the slab. The connections behaved elastically up to a rotation of approximately 0.005 rad. For the test of Specimen SU1 under a target gravity shear of 1/2, the maximum connection rotation was approximately 0.05 rad, which occurred at 4% drift, while a peak rotation of 0.065 rad was measured during the test under a 5/8 target gravity shear ratio. The response of Specimen SU2 was relatively similar to that of Specimen SU1 in terms of connection rotations. At 5% drift under a target gravity shear ratio of either 1/2 or 5/8, the maximum connection rotation was approximately 0.06 rad.

## Combined shear stresses due to direct shear and unbalanced moment

Shear stresses due to combined direct shear $V$ and unbalanced moment $M_{ub}$ were calculated using the "Eccentric Shear Model" in Section 11.11.7.2 of the ACI Building Code (ACI Committee 318 2008), which is based on the work by Di Stasio and Van Buren (1960), Moe (1961), and Hanson and Hanson (1968). In this model, the total shear stress in the connection is given by the summation of a shear stress due to direct shear $V$ and a shear stress due to eccentric shear, which is assumed to transfer a percentage $\gamma_v$ of the unbalanced moment $M_{ub}$ as follows

$$v = \frac{V}{A_c} \pm \frac{\gamma_v M_{ub} c}{J_c} \quad (1)$$

where $A_c$ is the area of the critical section of the connection; $\gamma_v = 0.4$ for the connections tested (ACI Committee 318 2008); $c$ is the distance, parallel to the loading direction, measured from the centroid of the critical section to the location under consideration; and $J_c$ is a section property, which is considered to be equivalent to the polar moment of inertia. As can be noted from Eq. (1), the distribution of shear stress transferring unbalanced moment is assumed to vary linearly along the length of the critical section parallel to the loading direction.

For Specimen SU1, the largest combined shear stress during the test under a target gravity shear ratio of 1/2 was equal to $0.36\sqrt{f_c'}$ (MPa) ($4.25\sqrt{f_c'}$ [psi]), calculated at 4% drift. For the test under a 5/8 target gravity shear ratio, the peak shear stress was $0.38\sqrt{f_c'}$ (MPa) ($4.57\sqrt{f_c'}$ [psi]), which was also calculated at 4% drift. For Specimen SU2, the peak combined shear stress under a target gravity shear ratio of 1/2 was slightly larger than that for Specimen SU1 $0.38\sqrt{f_c'}$ (MPa) ($4.61\sqrt{f_c'}$ [psi]), which was obtained at 4% drift. On the other hand, a peak shear stress of $0.34\sqrt{f_c'}$ (MPa) ($4.06\sqrt{f_c'}$ [psi]) was calculated at 3% drift under a 5/8 target gravity shear ratio. Peak shear stress in the following cycles decreased substantially, particularly due to the loss of connection stiffness and moment capacity.

## Connection shear stress versus rotation interaction

To evaluate the effect of reversals of inelastic rotations on connection punching shear strength and deformation capacity, the shear stress-rotation values at ultimate obtained from the tests of Specimens SU1 and SU2 were compared with those from the test of slabs under monotonically increased load described in the companion paper (Cheng and Parra-Montesinos 2010), (Fig. 11). These slab specimens

were S7 and S8, and S9 and S10 for fiber-reinforced concretes with a 1.5% volume fraction of regular strength and high-strength hooked steel fibers, respectively. It should be mentioned that the flexural reinforcement ratio in Specimens SU1 and SU2 (0.57%) was approximately equal to that in the slabs subjected to monotonic loading that exhibited substantial flexural yielding (Specimens S8 and S10), allowing the elimination of the effect of flexural reinforcement ratio on shear stress-rotation interaction for these four specimens. On the other hand, the reinforcement ratio in Specimens S7 and S9, which exhibited limited or no yielding prior to punching shear failure, was 0.83%.

In the specimens subjected to lateral displacement reversals, the maximum shear stress calculated from the eccentric shear model did not necessarily correspond to the maximum applied drift or connection rotation. In Specimen SU1, the maximum shear stress and rotation were observed at 4% drift and 5% drift, respectively, under a target gravity shear ratio of 5/8. Therefore, two values are shown in Fig. 11 along with the average value. In Specimen SU2, the maximum shear stress was calculated at 4% drift under a target gravity shear ratio of 1/2, whereas the maximum rotation occurred at 5% drift under a target gravity shear ratio of 5/8. These two values are also plotted in Fig. 11, along with the average value.

As shown in Fig. 11, the average peak shear stress-rotation value for Specimen SU1 and those for Specimens S9 and S10 indicate a nearly linear relationship between shear stress and slab rotation. Because no failure occurred in Specimen SU1, the data corresponding to this specimen may be taken as a lower bound. A similar trend can be seen when plotting the results for Specimens S7, S8, and SU2, but with a more pronounced decrease in strength with an increase in rotation. Overall, the test results shown in Fig. 11 indicate that under combined shear stresses less than or equal to (1/3) $\sqrt{f_c'}$ (MPa) ($4\sqrt{f_c'}$ [psi]), a rotation capacity of at least 0.05 rad may be expected in connections constructed with either of the two fiber-reinforced concretes evaluated.

### Influence of gravity shear ratio on drift capacity

To compare the effect of gravity shear ratio on drift capacity in the fiber-reinforced concrete specimens with that in regular concrete interior slab-column connections, Fig. 12 shows a plot of drift versus gravity shear ratio for Specimens SU1 and SU2, along with data from tests of reinforced concrete slab-column connections without shear reinforcement (Durrani and Du 1992; Hawkins et al. 1974; Islam and Park 1976; Pan and Moehle 1988; Robertson and Durrani 1990; Robertson and Johnson 2006; Robertson et al. 2002; Symonds et al. 1976; Wey and Durrani 1990; and Zee and Moehle 1984). Three points are shown for each of the two test specimens, corresponding to the connection shear ratios measured at 3, 4, and 5% drift. Except for the shear ratio at 5% drift for Specimen SU2, all data points correspond to the lateral displacement tests under a target gravity shear ratio of 5/8. It is worth mentioning that the connection of Specimen SU1 did not show any signs of distress throughout the test. Also, despite the damage sustained by the connection of Specimen SU2, it was capable of transferring the applied gravity load throughout the cycles corresponding to the data points shown in Fig. 12. Thus, it is conservative to take the data shown in the figure as the capacity of the test connections.

As shown in Fig. 12, the points corresponding to the two fiber-reinforced concrete specimens are located farther to the right and above other test data corresponding to similar failure drifts and gravity shear ratios, respectively. Thus, these data indicate that the use of either regular strength or high-strength hooked steel fiber reinforcement in a 1.5% volume fraction has the potential to substantially increase either punching shear strength, or drift capacity, or both compared to those observed in regular concrete slab-column connections. The limited test data indicate that for a gravity shear ratio of 1/2, a drift capacity of 4% can be expected, while a drift capacity of 5% would be expected for a gravity shear ratio of approximately 0.35.

## SUMMARY AND CONCLUSIONS

Results from the tests of two fiber-reinforced concrete slab-column connections under combined gravity load and lateral displacement reversals are presented. The connection of Specimen SU1 was reinforced with high-strength (2300 MPa [334 ksi]) hooked steel fibers in a 1.5% volume fraction, whereas regular strength (1100 MPa [160 ksi]) hooked steel fibers, also in a 1.5% volume fraction, were used in the connection of Specimen SU2.

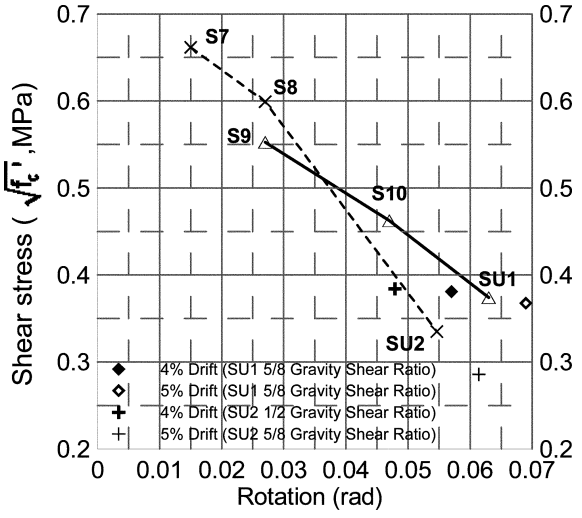


*Fig. 11—Shear stress versus rotation interaction. (Note: 1 MPa = 0.145 ksi.)*

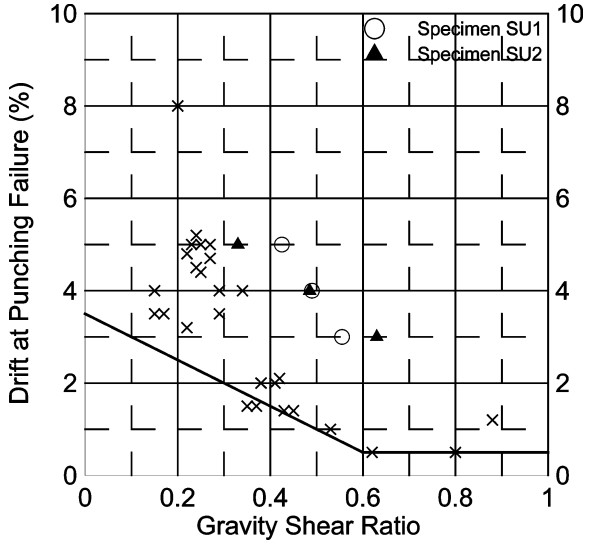


*Fig. 12—Drift capacity versus gravity shear ratio.*

From the results presented, the following conclusions can be drawn:

1. Steel fiber reinforcement is effective in increasing punching shear resistance and deformation capacity of slab-column connections under combined gravity load and lateral displacement reversals. The two test specimens were subjected to drift cycles of up to 5% drift and gravity shear ratios as high as 5/8. The peak connection shear stress demand was approximately $0.38\sqrt{f_c'}$ (MPa) ($4.6\sqrt{f_c'}$ [psi]) for both test specimens, calculated at 4% drift.

2. A combined shear stress due to direct shear and unbalanced moment of (1/3) $\sqrt{f_c'}$ (MPa) ($4\sqrt{f_c'}$ [psi]) represented a limit below which a rotation capacity of at least 0.05 rad can be expected in connections constructed with either of the two fiber-reinforced concretes evaluated. In terms of gravity shear ratio, the data suggest that a gravity shear ratio of 1/2 should be adequate for ensuring a drift capacity on the order of 4% drift.

## ACKNOWLEDGMENTS

This research was sponsored by the US National Science Foundation, as part of the Network for Earthquake Engineering Simulation (NEES) Program, under Grant No. CMS 0421180. The opinions expressed in this paper are those of the writers and do not necessarily express the views of the sponsor.

## REFERENCES

ACI Committee 318, 2008, "Building Code Requirements for Reinforced Concrete (ACI 318-08) and Commentary," American Concrete Institute, Farmington Hills, MI, 473 pp.

C 1609/C 1609M-05, 2005, "Standard Test Method for Flexural Performance of Fiber-Reinforced Concrete (Using Beam With Third-Point Loading), ASTM International, West Conshohocken, PA, 8 pp.

Cheng, M.-Y., and Parra-Montesinos, G. J., 2009, "Punching Shear Strength and Deformation Capacity of Fiber Reinforced Slab-Column Connections under Earthquake-Type Loading," *Report* UMCEE 09-01, Department of Civil and Environmental Engineering, University of Michigan, Ann Arbor, MI, 334 pp.

Cheng, M.-Y., and Parra-Montesinos, G. J., 2010, "Steel Fiber Reinforcement for Punching Shear Resistance in Slab-Column Connections—Part I: Monotonically Increased Load," *ACI Structural Journal*, V 107, No. 1, Jan.-Feb., pp. 101-109.

Corley, W. G., and Hawkins, N. M., 1968, "Shearhead Reinforcement for Slabs," ACI JOURNAL, *Proceedings* V. 65, No. 10, Oct., pp. 811-824.

Di Stasio, J., and Van Buren, M. P., 1960, "Transfer of Bending Moment between Flat-Plate Floor and Column," ACI JOURNAL, *Proceedings* V. 57, No. 9, Sept., pp. 299-314.

Diaz, A. J., and Durrani, A. J., 1991, "Seismic Resistance of Fiber-Reinforced Slab-Column Connections," *Report* No. 43, Structural Research at Rice, Rice University, Houston, TX, May, 144 pp.

Dilger, W.; Birkley, G.; and Mitchell, D., 2005, "Effect of Flexural Reinforcement on Punching Shear Resistance," *Punching Shear in Reinforced Concrete Slabs*, SP-232, M. A. Polak, ed., American Concrete Institute, Farmington Hills, MI, pp. 57-74.

Dilger, W. H., and Ghali, A., 1981, "Shear Reinforcement for Concrete Slabs," *Journal of Structural Division*, ASCE, V. 107, No. 12, pp. 2403-2420.

Durrani, A. J., and Du, Y., 1992, "Seismic Resistance of Slab-Column Connections in Existing Non-Ductile Flat-Plate Buildings," *Technical Report* NCEER-92-0010, National Center for Earthquake Engineering Research, State University of New York, Buffalo, NY, May, 75 pp.

Elstner, R. C., and Hognestad, E., 1956, "Shearing Strength of Reinforced Concrete Slabs," ACI JOURNAL, *Proceedings* V. 53, No. 1, Jan., pp. 29-58.

Hanna, S. N.; Mitchell, D.; and Hawkins, N. M., 1975, "Slab-Column Connections Containing Shear Reinforcement and Transferring High-Intensity Reversed Moments," *Report* SM 75-1, Division of Structures and Mechanics, Department of Civil Engineering, University of Washington, Seattle, WA, Aug., 94 pp.

Hanson, N. W., and Hanson, J. M., 1968, "Shear and Moment Transfer between Concrete Slabs and Columns," *Bulletin* D129, Development Department, Research and Development Laboratories, Portland Cement Association, Skokie, IL, 16 pp.

Hawkins, N. M.; Mitchell, D.; and Sheu, M. S., 1974, "Cyclic Behavior of Six Reinforced Concrete Slab-Column Specimens Transferring Moment and Shear," *Progress Report* 1973-74 on NSF Project GI-38717, Department of Civil Engineering, University of Washington, Seattle, WA, Sept., 50 pp.

Hueste, M. B. D., and Wight, J. K., 1997, "Evaluation of a Four-Story Reinforced Concrete Building Damaged During the Northridge Earthquake," *Earthquake Spectra*, V. 13, No. 3, pp. 387-414.

Hwang, S.-J., and Moehle, J. P., 1993, "An Experimental Study of Flat-Plate Structures under Vertical and Lateral Loads," *Report* No. UCB/EERC-93/03, Earthquake Engineering Research Center, University of California at Berkeley, Berkeley, CA, 278 pp.

Islam, S., and Park, R., 1976, "Tests of Slab-Column Connections with Shear and Unbalanced Flexure," *Journal of the Structural Division*, ASCE, V. 102, No. ST3, pp. 549-569.

Moe, J., 1961, "Shearing Strength of Reinforced Concrete Slabs and Footings under Concentrated Loads," *Bulletin* D47, Development Department, Research and Development Laboratories, Portland Cement Association, Skokie, IL, 130 pp.

Pan, A. A., and Moehle, J. P., 1988, "Reinforced Concrete Flat Plates under Lateral Loadings: An Experimental Study Including Biaxial Effects," *Report* No. UCB/EERC-88/16, Earthquake Engineering Research Center, University of California at Berkeley, Berkeley, CA, Oct., 262 pp.

Robertson, I. N., and Durrani, A. J., 1990, "Seismic Response of Connections in Indeterminate Flat-Slab Subassemblies," *Report* No. 41, Structural Research at Rice, Rice University, Houston, TX, July, 266 pp.

Robertson, I. N.; Kawai, T.; Lee, J.; and Johnson, G., 2002, "Cyclic Testing of Slab-Column Connections with Shear Reinforcement," *ACI Structural Journal*, V. 99, No. 5, Sept.-Oct., pp. 605-613.

Robertson, I. N., and Johnson, G., 2006, "Cyclic Lateral Loading of Nonductile Slab-Column Connections, *ACI Structural Journal*, V. 103, No. 3, May-June, pp. 356-364.

Symonds, D. W.; Mitchell, D.; and Hawkins, N. M., 1976, "Slab-Column Connections Subjected to High Intensity Shears and Transferring Reversed Moments," *Report* SM 76-2, Division of Structures and Mechanics, Department of Civil Engineering, University of Washington, Seattle, WA, Oct., 80 pp.

Wey, E. H., and Durrani, A. J., 1990, "Seismic Response of Slab-Column Connections with Shear Capitals," *Report* No. 42, Structural Research at Rice, Rice University, Houston, TX, Oct., 156 pp.

Zee, H. L., and Moehle, J. P., 1984, "Behavior of Interior and Exterior Flat Plate Connections Subjected to Inelastic Load Reversals," *Report* No. UCB/EERC-84/07, Earthquake Engineering Research Center, University of California at Berkeley, Berkeley, CA, Aug., 130 pp.